

PREDICTING OF WATER FILM THICKNESS AND VELOCITY FOR CORROSION RATE CALCULATION IN OIL-WATER FLOWS

Hua Shi, Hongbin Wang, W. Paul Jepson
NSF, I/UCRC Corrosion in Multiphase Systems Center
Department of Chemical Engineering
Ohio University
Athens, Ohio 45701

Lee D Rhyne
Texaco General Engineering Department
Bellaire, Texas 77402-0430

ABSTRACT

Experiments studying oil-water flows were conducted in a 10-cm diameter, 40-m long, horizontal pipeline. Oil (viscosity 3 cP at 25°C) and ASTM substitute seawater were used at superficial mixture velocities ranging from 0.4 to 3.0m/s. *in situ* water cut and *in situ* velocity along the pipe across section have been measured at a temperature of 25°C and a carbon dioxide partial pressure of 0.13 MPa for a whole range of water cut.

A novel mathematical segregated flow model, four-layer/phase was then developed for intermediate oil-water flow patterns of semi-segregated, semi-mixed and mixed as a three-phase model by incorporating experimental data. The mixed layer in the three-layer/phase model is further divided into water-in-oil (oil-continuous) and oil-in-water (water-continuous) layers by the phase inversion point. The experimental data are in good agreement with the predicted water film height from the model.

Keywords: corrosion, large diameter pipe, multiphase flow, oil-water flow, phase inversion, segregated flow model, three-layer/phase model, four-layer/phase model

INTRODUCTION

The simultaneous flow of oil and water in pipelines is a common occurrence in oil production systems, and occurs from the well perforations to the final stage of separation. As the well ages, the reservoir pressure decreases. To enhance oil recovery, water injection is commonly used to maintain reservoir pressure. Meanwhile, as the oil saturation decreases, an increasing amount of water seeps into the well from the surroundings. Thus, the water fraction will tend to increase over the productive life of the well and the water cuts can be up to 99%, and many wells are now operated at water cuts as high as 80%. Therefore, the possibility of corrosion in oil-water flows is very high.

It is well known that injection of corrosion inhibitors is most widely used of all the methods of curbing corrosion in multiphase. The effectiveness of the inhibitor depends on the pipeline material, the inhibitor composition and flow conditions. To be effective, the inhibitor must be introduced into the phase in contact with the pipe wall. The decision on whether to use oil or water soluble inhibitors, amount of inhibitor can be made effectively, only if flow patterns and phase distributions under different flow conditions are known.

Gas-liquid flows have been extensively studied. Even in the studies of gas-oil-water systems, the two liquid phases are almost always treated as a single mixed fluid. Research works have shown that the flow characteristics of oil-water mixtures are significantly different from the gas-liquid systems. These differences arise mainly from the much smaller differences in density and viscosity, compared to the gas-liquid flows. The density ratio of the fluids is typically in the range of 0.7~1.1, compared with values of 0.001~0.2 for gas-liquid systems¹. The flow of oil-water mixtures within a pipeline is highly complex due to the slip between oil and water, similar to the slip between gas and liquid, and the formation of dispersions or emulsions, different from gas-liquid flows. Understanding the distinctive features in oil-water flows is extremely important for predicting corrosion in oil-water pipelines. However, very few studies have been performed on pipeline flows of two immiscible liquid phases. The research work on corrosion in oil-water flows has been even sparser.

Flow Pattern

The various transfer mechanisms between two phases depend on the flow patterns or flow regimes. This leads to the use of regime dependent correlation. Oil-water flow patterns are very important because it indicates the relative amount of each phase coating the pipe wall, position of the phases and the degree of mixing during flow.

Oil-water flows have been studied following the ways of gas-liquid studies. Therefore, most researchers have emphasized flow pattern concept on. Figure 1 shows several classical oil-water flow patterns observed by Oglesby². The segregated flow regime is defined as the flow of the liquids in two distinct layers, with no mixing at the interface. As the mixture velocity is increased, some mixing occurs at the interface giving rise to semi-segregated flow. The flow is said to be semi-mixed when there is a segregated flow of a dispersion and a 'free' phase and the dispersion volume is less than half the total pipe volume. Mixed flow occurs when the oil-water dispersion occupies more than half the pipe volume. At high mixture velocity, oil and water are totally mixed. When some sharp steep gradient of fluid concentration in the mixture are incurred, the flow pattern is termed semi-dispersed. The oil and water become fully dispersed and the mixture flows as a homogeneous phase without appreciable changes in concentration in pipeline. Shi³ has also observed these six flow patterns.

Cox Jr.⁴ conducted his experiment in a 5.08 cm pipe using a wide range of oil and water flow rates and involving inclination angles of 0, -15, and -30 degrees from horizontal. He observed greatly

different flow regimes in oil-water flow from the flow regimes encountered with gas-liquid flow, and he reported that there existed no meaningful correlation when comparing experimental flow regime data with modified and established gas-liquid dimensionless parameters.

Trallero et al.⁵ observed flow patterns in a 5.08 cm ID straight pipe using a refined oil with a viscosity of 28 cP and a density of 884 kg/m³. The oil-water flows are classified in two categories: segregated flow and dispersed flow. Segregated flow patterns include the stratified flow and stratified flow with some mixing at the interface. These correspond to the segregated flow and semi-segregated flow by Oglesby. Four flow patterns have been characterized in dispersed flow: oil in water and water, oil in water emulsion, water in oil and oil in water, and water in oil emulsion.

Corrosion Rate

Prediction of corrosion rates in oil-water flows requires knowledge of the *in situ* holdup and velocity of the water layer to predict mass transfer coefficient. Oil/water composition affects the corrosion rate. Kanwar and Jepson⁶ performed experiments in 10 cm internal diameter horizontal pipeline, and found the distribution of the phases is very important. At oil compositions from 0 to 60%, the oil/water mixture separated and a water layer flowed along the bottom of the pipe with the oil flowing above it. An increase in oil concentration up to 60% led to an increase in corrosion rates. Above an oil concentration of 60%, when the phases became well mixed with oil being the continuous phase, the corrosion rates were lower.

It is well known that in multiphase flows, the actual velocities of the individual phases are, in general, not the same and usually do not correspond to their velocities at inlet conditions due to the slip between the phases. Higher viscosity oil is observed to move slower than water. Meanwhile, some researchers believe that under most oil-water flow situations, the oil phase flows faster than the water phase resulting in accumulation or holdup of water⁷. It is highly desirable to be able to accurately predict the *in situ* velocity of the water layer.

An initial attempt at a mechanistic model was developed to predict the hold up and pressure drop in semi-stratified, semi-mixed and semi-dispersed flows by Vedapuri⁸. In most oil-water flow cases, even in a condition of a relatively high velocity, there is an oil layer and a water layer, and an oil/water mixture layer. Therefore, as shown in Figure 2, oil-water flow has been treated as a three phase stratified flow with a water layer at the bottom, an oil layer at the top and a mixed layer, which is an oil-water dispersion, at the center of the pipe. With an increase in mixture velocity, the thickness of water and oil layers decrease while that of the mixed layer increases. The predicted water film thickness was found to be in good agreement with the experimental data. However, he did not consider one of the most important features of oil-water flow, phase inversion.

Phase Inversion

One phenomenon that makes oil-water dispersion flow different from other types of two-phase flows is the phase inversion⁹. In oil-water flows, increasing the concentration of the "dispersed" phase beyond a certain critical point causes it to become the "continuous" phase, and the other to become the "dispersed" phase. This phenomenon is called phase inversion. The critical water percentage for water to become the continuous phase is usually called phase inversion point.

Ariachakaran et al.⁹ explained how the phase inversion process takes place by using a figure similar to that of Figure 3. It shows that as the water droplets become more concentrated and start to coalesce, the water becomes the continuous phase and the inversion occurs at the maximum apparent

viscosity. Once past the inversion point, the apparent viscosity drops significantly due to the water becoming the continuous phase. They showed that as the oil viscosity increases, the oil-continuous fluid could retain more water as droplets before the mixture reaches the inversion point.

Phase inversion is of special importance in oil-water flows because it provides the information of the onset of corrosion and subsequent using corrosion inhibitor chemicals. Inhibitors are usually oil or water-soluble and need that phase to be continuous phase for the inhibitor to work effectively. Meanwhile, when the "dispersed" phase becomes the "continuous" phase and vice versa, a large increase in the pressure drop is noticed. Therefore, the phase inversion phenomenon impacts the pipeline design.

The sharp increase in pressure drop is attributed to the increase in the effective mixture viscosity observed around the inversion point, meaning that the mixture has a higher viscosity than the following mixing equation predicts:

$$\mu_m = \mu_w \eta_w + \mu_o (1 - \eta_w) \quad (1)$$

where,

μ_m = viscosity of oil-water mixture

μ_w = viscosity of water

η_w = volume fraction of water

μ_o = viscosity of oil

The effective mixture viscosity can become greater than viscosity of either the water or the oil. The maximum in the effective mixture viscosity always occurs at the inversion point. Thus, if the fluid is well mixed and almost uniform, then the pressure drop will reach a maximum at the inlet water cut corresponding to the inversion point of the system. If the fluid is not uniform from the top to the bottom of the pipe, then the maximum in pressure drop may not occur at the inlet water cut corresponding to the inversion point.

Research Objectives

Vedapuri's three-phase segregated model is a very useful tool for predicting the water holdup and pressure gradient in pipelines. However, in any case of semi-segregated, semi-mixed and mixed flows, the mixed layer is not homogeneous. Considering the phase inversion phenomenon, starting at the top of the pipe, it can be deduced that there are at least 4 kinds or layers of fluids: pure oil, water-in-oil phase, oil-in-water phase, and pure water. It should be noted that this situation is not contrary to the three layer segregated flow model when the phase inversion is considered because the mixed layer is actually divided into oil-in-water and water-in-oil layers by the phase inversion point as shown in Figure 4.

Furthermore, one of the most important aspects here, for corrosion prevention in oil-water flows, it is well known water layer and oil-in-water/water-continuous layer both contribute to the corrosion. Therefore, the water film height for predicting the corrosion rate should actually be the pure water layer's height plus the water-continuous layer's thickness. In this point of view, the four-layer model provides information, which the three-phase model can not.

Trallero's⁵ dual dispersion flow pattern i.e. oil-in-water and water-in-oil dispersions flowing together can also be considered as a four-phase segregated flow model since generally, for many kinds of oil, both of the dispersions are not homogeneous nor even close to homogeneous. The oil-in-water dispersion thus can be divided into a pure water-dominant phase and an oil-in-water dispersion phase, while the water-in-oil dispersion can be divided into a pure oil-dominant phase and a water-in-oil

dispersion phase. On the other hand, with oil like what Trallero used, it is easy to form the dual dispersion flow pattern. If combining the pure water layer with the water continuous layer to a oil-in-water layer and meantime, combining the pure oil layer with the oil-continuous layer to a water-in-oil layer, the four-phase segregated model can be simplified to Jayawardena's¹⁰ dual dispersion flow model. Therefore, the four-phase segregated flow model gives a relatively comprehensive description of most cases of oil-water flows, and thus is more useful and powerful in predicting the behavior of oil-water flows in pipelines.

Experiments were performed to measure water holdup, velocity profiles, and phase inversion point. The data are then incorporated into a four-phase segregated model similar to Vedapuri's three-phase segregated model. The model predicts the phase distribution, *in situ* holdup, and velocity used to calculate corrosion rate in oil-water flows.

EXPERIMENTAL PROCEDURE

The overall layout of the pipe system is shown in Figure 5. A 40 m long, 10.1 cm inner diameter, low pressure (13 MPa), low temperature (60°C), inclinable acrylic pipe flow loop was used in the study of oil-water flows. The oil-water mixture with specified composition is placed in a 1.2 m³ stainless storage tank (A). The tank is equipped with two 1 kW heaters (B). The oil-water mixture from the storage tank is pumped into a 7 m long, 7.5 cm PVC pipeline using a 5hp centrifugal pump (C). The flow rate is controlled within a range of 0 to 3 m/s with a combination of the variable speed pump and a by-pass system (D), which also serves to agitate the oil-water mixture in the tank to ensure well-mixed flow. An orifice plate, which has been calibrated by flowing oil-water mixture at different water cuts, is used to measure flow rate. A T-junction fitted with a ball valve is set as a sampling valve, present at the exit of the pump. Liquid samples are withdrawn at regular intervals from this junction, before the start of the experiments and while the experiment is in progress, to ensure the flowing water percentage is maintained. Carbon dioxide from a storage tank (E) is introduced into the system to maintain the pressure. The oil-water mixture and carbon dioxide meet at mixing tee (H), the multiphase mixture passes through a 10.16 cm ID, 2 m long flexible hose (G) and enters the 18 m long and 10.1 cm I.D Plexi-glass section where the test section is installed. The multiphase mixture then enters a similar downward section and returns to the tank.

The test section is a 2 m long, 10 cm I.D. plexiglas pipe as shown in Figure 6. At pipe ports A, flush mounted Electrical Resistance (ER) probes are installed to measure the corrosion rate. A special conductance probe was used to determine the phase inversion points at port B. There is a remarkable difference in the capacitance reading between the oil continuous and the water continuous phase. The phase inversion point for this oil-water system is around 45%. A sampling tube (D) is used to measure the local water concentration and determine the water film height at port C. The *in situ* velocity profile across the vertical diameter is determined using a Pitot tube (D) at port C. The set of two pressure taps (E) are 3.76 m apart is used to measure the pressure drop. The system's temperature is monitored by a thermocouple (F).

MODEL DEVELOPMENT

As shown in Figure 4, oil-water flows are described as four segregated phases. The model assumes that both the oil-in-water and the water-in-oil phase are a homogeneous pseudo phase, with a uniform density and viscosity, and with no slip between the two phases in the dispersion. The dispersion

is also assumed to behave in a Newtonian way. The four-phase segregated flow model is for oil-water flows in horizontal and near horizontal pipelines. This model predicts the water film height (H_1), as well as four layer's velocity.

The method for developing the four-phase model is the same as Vedapuri's by considering the momentum and mass balance of the each phase. A momentum balance is carried out for the oil, water and mixture layers as follows

For the water layer

$$-A_w \left(\frac{dp}{dx} \right) - \tau_w S_w - \tau_{i1} S_{i1} - \rho_w A_w g \sin \alpha = 0 \quad (2)$$

For the oil-in-water layer

$$-A_{MW} \left(\frac{dp}{dx} \right) - \tau_{MW} S_{MW} - \tau_{i1} S_{i1} + \tau_{i2} S_{i2} - \rho_{MW} A_{MW} g \sin \alpha = 0 \quad (3)$$

For the water-in-oil layer

$$-A_{MO} \left(\frac{dp}{dx} \right) - \tau_{MO} S_{MO} - \tau_{i2} S_{i2} - \tau_{i3} S_{i3} - \rho_{MO} A_{MO} g \sin \alpha = 0 \quad (4)$$

For the oil layer

$$-A_o \left(\frac{dp}{dx} \right) - \tau_o S_o + \tau_{i3} S_{i3} - \rho_o A_o g \sin(\alpha) = 0 \quad (5)$$

where, the subscripts w, mw, mo and o refer to the water, oil-in-water layer (mixed water), water-in-oil (mixed oil), and the oil layer respectively. The subscript i1, i2, and i3 denote the water-mixture interface and mixture-oil interface.

Removing the pressure drop term from 2 and 3 yields,

$$\tau_w \frac{S_w}{A_w} - \tau_{MW} \frac{S_{MW}}{A_{MW}} + \tau_{i2} \frac{S_{i2}}{A_{MW}} - \tau_{i1} \left(\frac{S_{i1}}{A_w} + \frac{S_{i1}}{A_{MW}} \right) + (\rho_w - \rho_{MW}) g \sin(\alpha) = 0 \quad (6)$$

similarly, from 3 and 4,

$$\tau_{MW} \frac{S_{MW}}{A_{MW}} - \tau_{MO} \frac{S_{MO}}{A_{MO}} - \tau_{i3} \frac{S_{i3}}{A_{MO}} + \tau_{i1} \frac{S_{i1}}{A_{MW}} - \tau_{i2} \left(\frac{S_{i2}}{A_{MW}} + \frac{S_{i2}}{A_{MO}} \right) + (\rho_{MW} - \rho_{MO}) g \sin(\alpha) = 0 \quad (7)$$

and, from 4 and 5,

$$\tau_o \frac{S_o}{A_o} - \tau_{MO} \frac{S_{MO}}{A_{MO}} - \tau_{i2} \frac{S_{i2}}{A_{MO}} - \tau_{i3} \left(\frac{S_{i3}}{A_o} + \frac{S_{i3}}{A_{MO}} \right) + (\rho_o - \rho_{MO}) g \sin(\alpha) = 0 \quad (8)$$

Following Taitel and Dukler¹¹, the shear stresses are evaluated by using a Blasius type equation as shown in the following:

$$\tau_w = f_w \frac{\rho_w U_w^2}{2} \quad \tau_{MW} = f_{MW} \frac{\rho_{MW} U_{MW}^2}{2} \quad \tau_{MO} = f_{MO} \frac{\rho_{MO} U_{MO}^2}{2} \quad \tau_o = f_o \frac{\rho_o U_o^2}{2} \quad (9)$$

$$\begin{aligned}\tau_{i1} &= f_{i1} \frac{\rho (U_{MW} - U_M)(U_{MW} - U_M)}{2} & \tau_{i2} &= f_{i2} \frac{\rho (U_{MW} - U_{MO})(U_{MW} - U_{MO})}{2} \\ \tau_{i3} &= f_{i3} \frac{\rho (U_O - U_{MO})(U_O - U_{MO})}{2}\end{aligned}\quad (10)$$

where,

$\frac{dP}{dx}$ = pressure gradient

A_W, A_O, A_{MW}, A_{MO} = cross sectional area occupied by the water, oil, oil-in-water, and water-in-oil layer

τ_W, τ_O = shear stress at wall for water and oil layer

$\tau_{i1}, \tau_{i2}, \tau_{i3}$ = interfacial shear stress

S_W, S_O, S_{MW}, S_{MO} = portion of pipe circumference of the water, oil, oil-in-water, and water-in-oil layer

S_{i1}, S_{i2}, S_{i3} = width of the interface

$\rho_W, \rho_O, \rho_{MW}, \rho_{MO}$ = average density of the water, oil, oil-in-water, and water-in-oil layer

α = pipe inclination from horizontal

f_W, f_O, f_{MW}, f_{MO} = friction factors for water, oil, oil-in-water, and water-in-oil, layer

f_{i1}, f_{i2}, f_{i3} = interfacial friction factor

The friction factors are evaluated using an approach similar to Brauner and Maron¹².

Meanwhile, a mass balance can be carried out for four layers as follows:

$$Q_{TW} = Q_W + \eta_M Q_M \quad (11)$$

$$Q_{TO} = Q_O + (1 - \eta_M) Q_M \quad (12)$$

$$Q_{TMW} = \eta_{MW} Q_{MW} + \eta_{MO} Q_{MO} \quad (13)$$

$$Q_{TMO} = (1 - \eta_{MW}) Q_{MW} + (1 - \eta_{MO}) Q_{MO} \quad (14)$$

and from above four equations, the superficial velocities can be derived as,

$$U_{SWinput} = U_{SW} + \eta_M U_{SM} \quad (15)$$

$$U_{SOinput} = U_{SO} + (1 - \eta_M) U_{SM} \quad (16)$$

$$U_{STW} = \eta_{MW} U_{SMW} + \eta_{MO} U_{SMO} \quad (17)$$

$$U_{STO} = (1 - \eta_{MW}) U_{SMW} + (1 - \eta_{MO}) U_{SMO} \quad (18)$$

where

$Q_W, Q_O, Q_{TW}, Q_{TO}, Q_{MW}, Q_{MO}$ = volume flow rate of the pure water, pure oil, total water, total oil, oil-in-water, and water-in-oil layer

$\eta_M, \eta_{MW}, \eta_{MO}$ = water concentration in the mixed, oil-in-water, and water-in-oil layer

$U_{SWinput}, U_{SOinput}$ = superficial velocity of the input water, and input oil

$U_{SW}, U_{SO}, U_{SM}, U_{STM}, U_{STO}, U_{SMW}, U_{SMO}$ = superficial velocity of the water, oil, mixed, total water, total oil, oil-in-water, and water-in-oil layer

To solve the momentum and the mass balance equations simultaneously, the number of equations must equal the number of unknowns. In the above seven equations, there are eleven unknowns: U_{SW} , U_{SO} , U_{SM} , U_{SMW} , U_{SMO} , η_M , η_{WM} , η_{WO} , A_M , A_{MW} and A_{MO} . Thus four more equations need to be developed.

The phase inversion point in this oil-water system has been measured to be around 45%¹³. This value is used to divide the mixed layer into the oil-in-water and water-in-oil layer. An assumption is made that both the oil-in-water and water-in-oil phases are homogeneous. The mixture density and viscosity then can be calculated. Note here that mixture viscosity was calculated using a correlation author developed based on Brinkman's^{13, 14}.

After the compositions of the oil-in-water and water-in-oil layer, η_{WM} and η_{WO} have been found, only two more equations are needed. It has been found the composition of the mixed layer (oil-in-water layer + water-in-oil layer) is between the input water cut and 50%¹⁴. Also, the *in situ* velocity of the mixed layer travels approximately 1.15 times the input mixture velocity for most of the cases¹⁴. Hence, the two closure equations are:

$$\begin{aligned} \eta_M &= \eta_{input} \sim 50\% & \text{for } \eta_{input} \leq 50\% \\ \eta_M &= 50\% \sim \eta_{input} & \text{for } \eta_{input} > 50\% \end{aligned} \quad (19)$$

and,

$$\begin{aligned} U_{sm} &= 0.9 * (U_{SW} + U_{SO}) & \text{for } \eta_{input} < 30\% \\ U_{SM} &= 1.1 \sigma_{int}^{-0.015} (U_{SW} + U_{SO}) & \text{for } \eta_{input} \geq 30\% \end{aligned} \quad (20)$$

RESULTS & DISCUSSION

The model predicts the thickness and *in situ* velocity of the each layer given the pipe diameter, oil and water properties, input superficial velocities and input composition. The results of pure water film height, water (pure + water continuous) layer height, and the mixed layer thickness are shown in Figure 7 ~ Figure 14 as a function of input mixture velocity. The mixture velocity is measured from orifice plate. A ± 3 mm error bar for experimental data is present in the Figures.

Figure 7 and 8 shows the variation of the water layer's thickness with input mixture velocity for four different input water cuts. It can be seen that the thickness of the water layer decreases with an increasing input mixture velocity. From Figure 7 at a 20% water cut, the experimental water film height decreases from 0.3 to 0.12 when the mixture velocity is increased from 0.6 to 1.4 m/s. The predicted value is from 0.28 to 0.16. For the input water cut of 40%, the experimental data range from 0.44 to 0.15 and the model gives value from 0.43 to 0.19. It can be seen that the predicted values are very close to the experimental values.

Increasing the input cut to 60% and 80%, the change in the water layer height is seen in Figure 8. As the input mixture velocity is increased from 0.6 to 1.4 m/s, the water layer thickness decreases from 0.54 to 0.30 for 60% water cut and from 0.69 to 0.45 for 80% water cut. The predicted value decreases from 0.52 to 0.33 and 0.65 to 0.50 respectively. Again, the model results agree well with the experimental data.

The mixed layer thickness results are shown in Figure 9 and 10. The model predicts the trend that the mixed layer increases with an increase in mixture velocity well. For input water cut of 20% and

40% as shown in Figure 9, the experimental mixed layer thickness increases from 0.02 to 0.30 and 0.03 to 0.58 respectively as the mixture velocity increases from 0.6 m/s to 1.4 m/s, and the predicted value increases from 0.07 to 0.25 and 0.07 to 0.54 respectively. Similar trends are shown for 60% and 80% input water cuts in Figure 10. Here, it is seen that the difference between the experimental and predicted values is relatively larger here. This is because that the mixed layer thickness is obtained by subtraction of two heights ($H_2 - H$, see Figure 4), so the error can be doubled as 0.06 dimensionless height. It is also seen that the model slight under predicts the mixed layer values. However, the location of the interface cannot be defined to less than approximately 4 mm due to the presence of waves. Therefore, the predicting results are reasonable. From Figure 9 and 10, it can be clearly seen that 40% input water cut has a thicker mixed layer than the other input water cut as observed in experiments. This is due to that 40% input water is very close to the phase inversion point at 45% water.

Figure 11 and 12 shows the variation of the total water film thickness with input mixture velocity. For input water cuts of 20% and 40% in Figure 11, the total water height decreases from 0.3 to 0.23 and 0.45 to 0.33 respectively. The predicted values are from 0.32 to 0.27 and 0.43 to 0.36 respectively. A completely different trend is shown in Figure 12 at higher input water cuts of 60% and 80%. The total water film height increases with the mixed velocity. The experimental data are from 0.55 to 0.65 and 0.70 to 0.77, and the predicted values are from 0.56 to 0.66, and from 0.70 to 0.76 respectively. The different trends for total water film height at different water cuts are due to phase inversion phenomena. The homogeneous mixture of oil and water has a water composition of the input water cut and it is between the water and oil layer. When the input water cuts (20% & 40%) are below the phase inversion point (45%), the total water height is below the mixed layer and decreases with the input mixture velocity, while the higher (60% & 80%) input water cuts than the inversion point behave in opposite way for the same reason. The fact that the model can predict this trend shows that the predictive capability of the model is rather good.

Figure 13 and 14 combines the results from Figure 7, 8, 11, and 12, and shows the comparison of the pure water film height and total water film height. As seen in the Figure 13 for the input water cuts of 20% and 40%, there is a large distance between the pure and total water film height. For the 60% and 80% input water in Figure 14, even the trends of the film height for pure water and total water are different. Figure 13 and 14 not only give the concept that big differences between the pure and total water film height, but also indicate the big error on corrosion prediction when using only the pure water film height instead of the total water film height. This shows the much more valuable of the four-phase model over the three-phase model.

CONCLUSIONS

- *In situ* water holdup and velocity are strongly affected by input water cut, superficial mixture velocity. Phase inversion point is around 45% of water for the system investigated.
- Four-phase segregated flow model is especially practical for predicting corrosion behavior in oil-water flows because the total water film thickness is needed. The predicted water film height from model has been compared with the experimental data and the agreement between and experimental values is good.
- The three and four-phase/layer models can not predict water drop out from oil/water dispersion or emulsion in oil-water flows and mostly work for input water cut range from 10 ~ 90%. A multi-layer mechanistic model has been developed by using a commercial CFD simulator CFX¹⁵. The model is of great significance for predicting water drop out and thus to predict the onset of corrosion.

ACKNOWLEDGMENTS

Author would like to thank the financial support from the Advisory Board companies of NSF, I/UCRC Corrosion in Multiphase Systems Center. A graduate fellowship from Texaco for Hua Shi is also gratefully appreciated.

REFERENCES

1. Simmons, M.J.H., and Azzopardi, B.J., "Drop Size Distributions in Dispersed Liquid-Liquid Pipe Flow", *Int. J. Multiphase Flow*, **27**, 843-859, 2001.
2. Oglesby, K. D., "An Experimental Study on the Effects of Oil Viscosity, Mixture Velocity and Water Fraction on Horizontal Oil-Water flow", M.S. Thesis, University of Tulsa, 1979.
3. Shi, H., Cai, J.Y. and Jepson, W. P., "The Effect of Surfactants on Flow Characteristics in Oil/Water Flows in Large Diameter Horizontal Pipelines", *Multiphase* **99**, 181-199, 1999.
4. Cox Jr., A.L., "A Study of Horizontal and Downhill Two-Phase Oil-Water Flow", M.S. Thesis, The University of Texas at Austin, 1985.
5. Trallero, J. L, Sarica, C and J. P. Brill, "A Study of Oil-Water Flow Patterns in Horizontal Pipes", *SPE*, Paper No. 36609, 363-375, 1996.
6. Kanwar, S. and Jepson, W. P., "A Model to Predict Sweet Corrosion of Multiphase Flow in Horizontal Pipelines", *Corrosion/94*, paper no 24, 1994
7. Flores, J. G., Sarica, C., Chen, T. X., and Brill, J. P., "Investigation of Holdup and Pressure Drop Behavior for Oil-Water Flow in Vertical and Deviated Wells", *ETCE-98*, Paper No. 10797, 1997.
8. Vedapuri, D., Bessette, D. and Jepson, W. P., "A Segregated Flow Model to Predict Water Layer Thickness in Oil-Water Flows in Horizontal and Slightly Inclined Pipes", *Multiphase* **97**, 75-105, 1997.
9. Arirachakaran, S., K. D., Oglesby, M. S., Malinovsky, M.S., Shoham, O., and J.P. Brill, "An Analysis of Oil-Water Flow Phenomena in Horizontal Pipes", *SPE* paper 18836, 155-167, 1989.
10. Javawardena, S. S., Alkaya, B., Redus, C. L., and Brill, J. P., "A New Model for Dispersed multi-layer Oil-Water Flows", *Multiphase* **2000**, 77-89, 2000.
11. Taitel, Y., and Dukler, A.E., "A Model for Prediction Flow Regime Transitions in Horizontal and Near Horizontal Gas-Liquid Flows", *AIChE J.*, **22**, No.1, 47-55, 1976.
12. Brauner, N., and Maron, D. M., "Two Phase of Liquid-Liquid Stratified Flow", *PCH* **11**, No.4, 487-506, 1989.
13. H. Shi, "A Study of Oil-Water Flows in Large Diameter Horizontal Pipelines", Ph.D Dissertation, Ohio University, July 2001.
14. Brinkman, H.C., "The Viscosity of concentrated Suspensions and Solutions", *Phys. Chem. Hydrodynamics*, **11**, 487-506, 1952.
15. Rhyne, Lee (Texaco), "Oil - Water Mechanistic Model", Advisory Board Meeting, NSF I/ UCRC Corrosion in Multiphase Systems Center, Athens, Ohio, Oct, 2000.

Segregated – no mixing at the interface

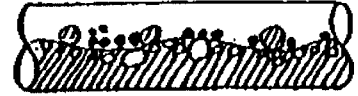
Semi-segregated – some mixing at the interface

Semi-mixed – segregated flow of a dispersion and a “free” phase. Bubbly interface. Dispersion volume less than half of the total pipe volume

Mixed – same as the above but with the dispersion occupying over half of the total pipe volume

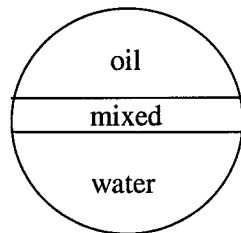
Semi –dispersed – some vertical gradient of fluid concentration in the mixture

Homogeneous – fully dispersed homogeneous flow

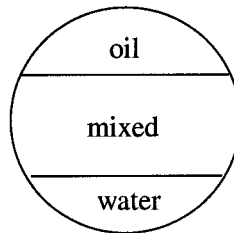


Flow Direction →

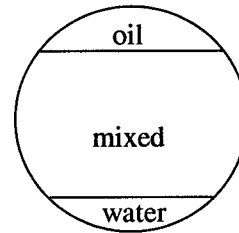
Figure 1 Flow pattern classifications for oil-water flows (Oglesby, 1979)



Semi-Stratified



Semi-Mixed



Semi-Dispersed

Figure 2 Cross section for three-phase flow patterns (Vedapuri, 1997)

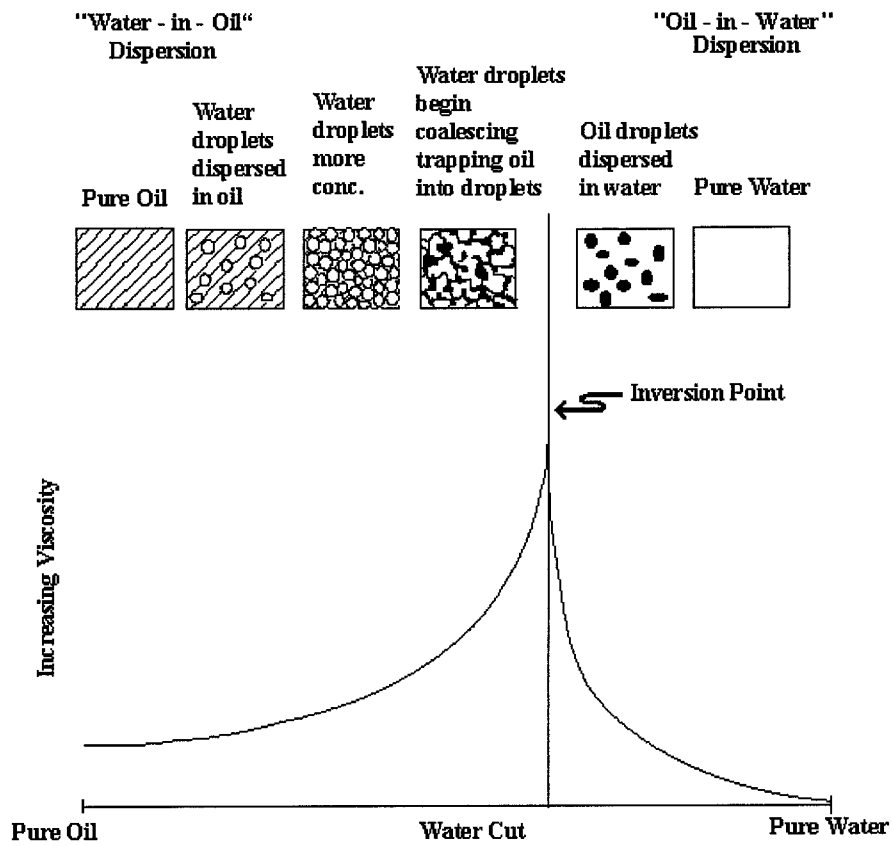


Figure 3 Phase inversion process for oil-water dispersion flow (modified from Arirachakaran's, 1989)

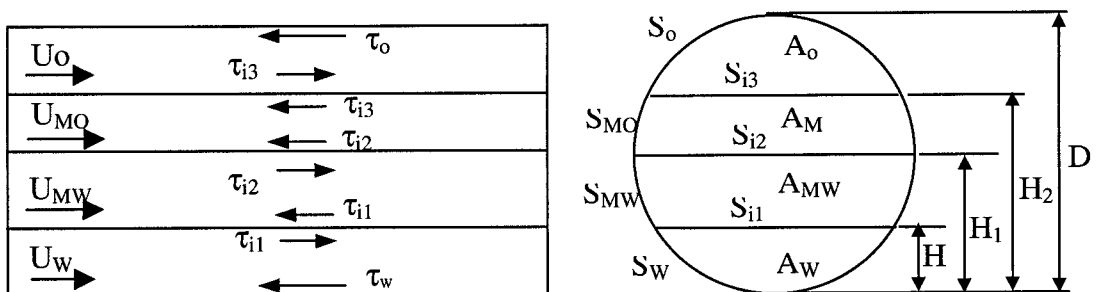


Figure 4 Schematic representation of the four-phase segregated oil-water flow

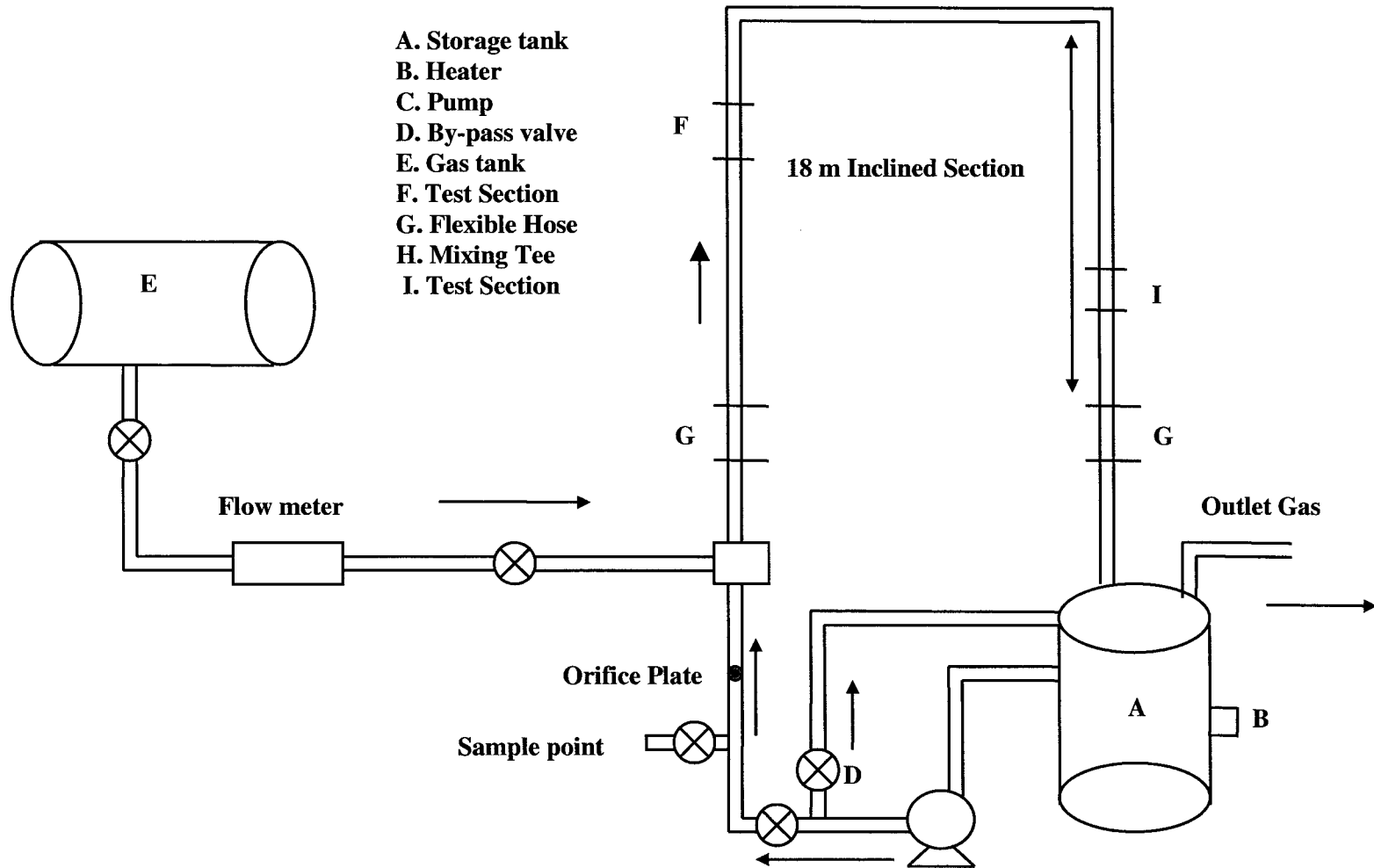


Figure 5 Experimental layout of flow loop

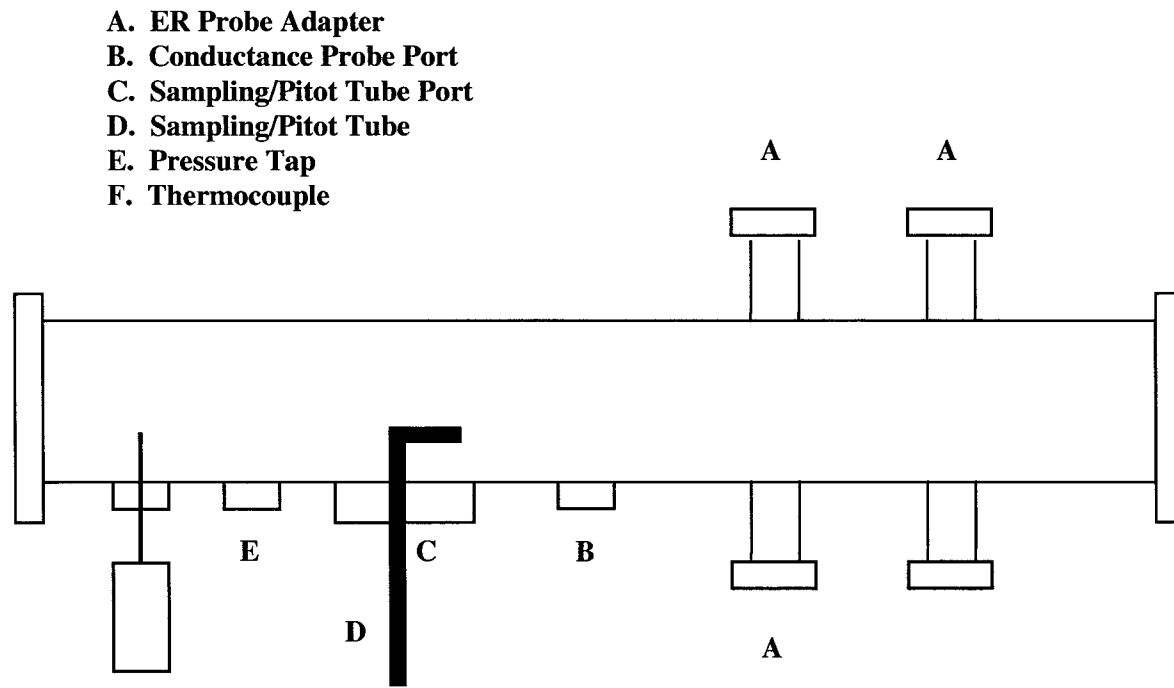


Figure 6 Test section

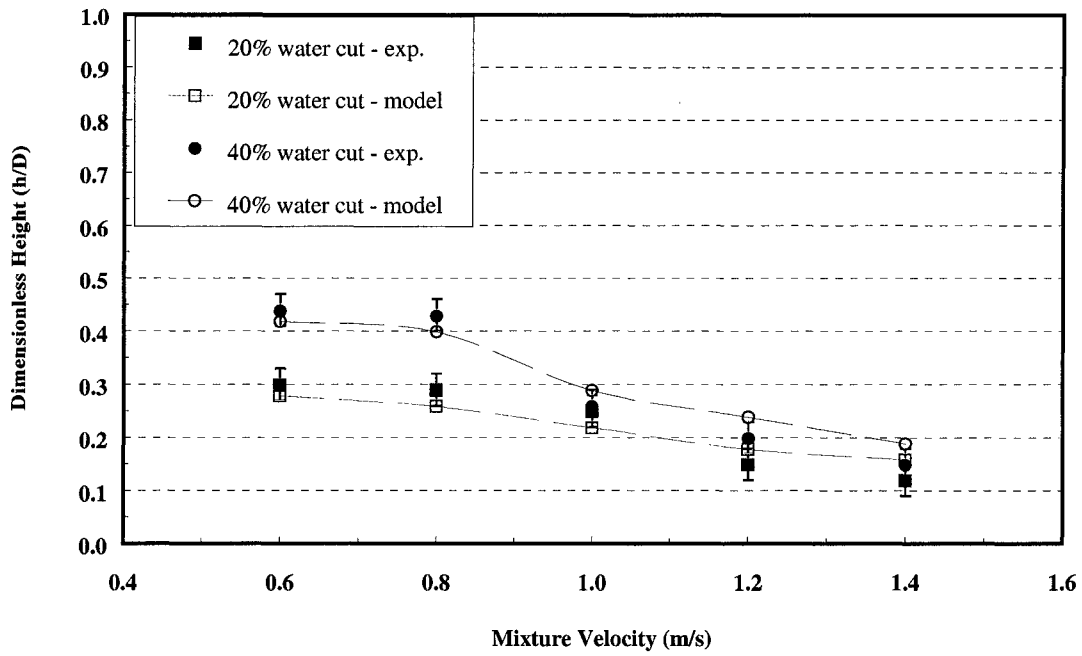


Figure 7 Variation of water layer height with velocity

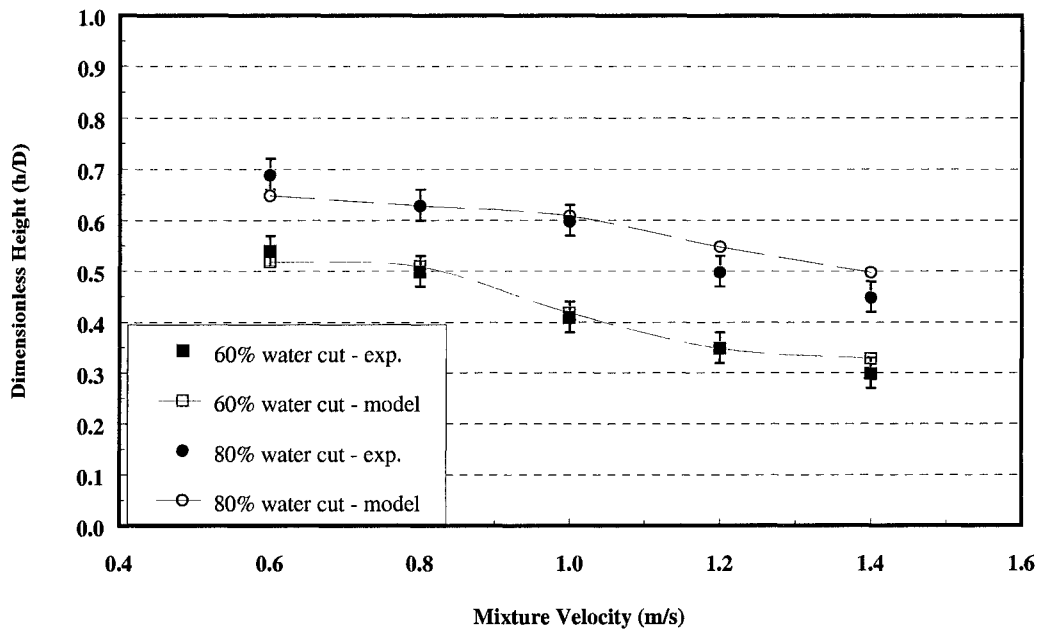


Figure 8 Variation of water layer height with velocity

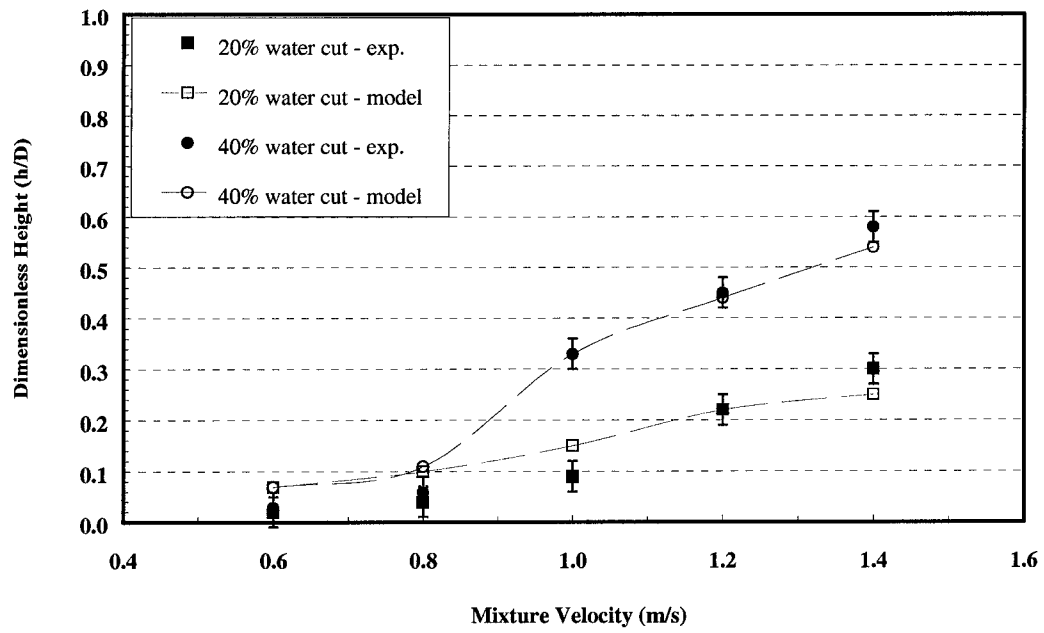


Figure 9 Variation of mixed layer thickness with velocity

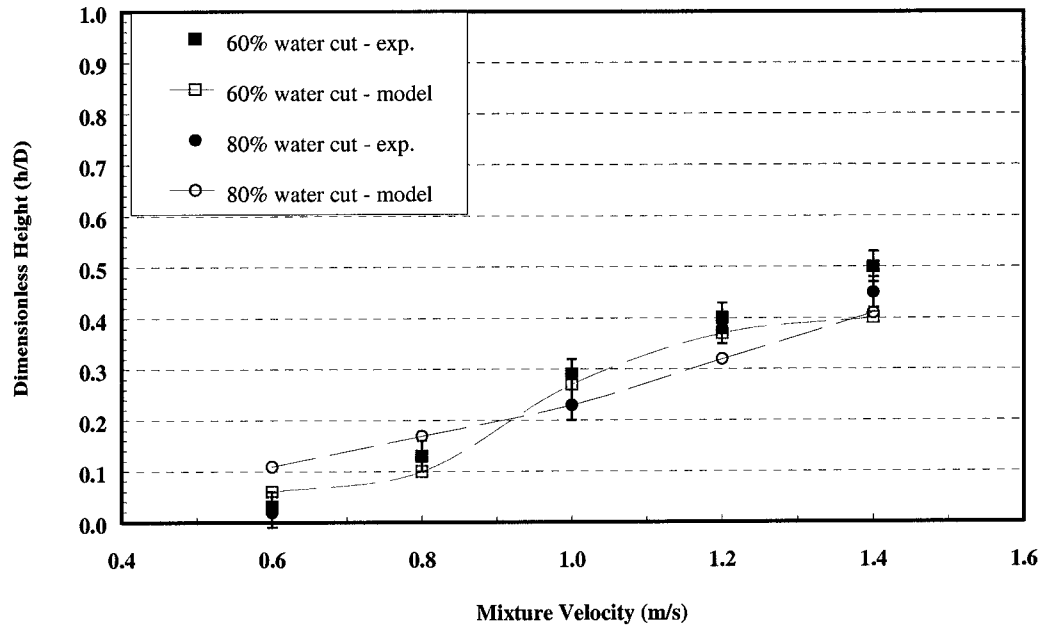


Figure 10 Variation of mixed layer thickness with velocity

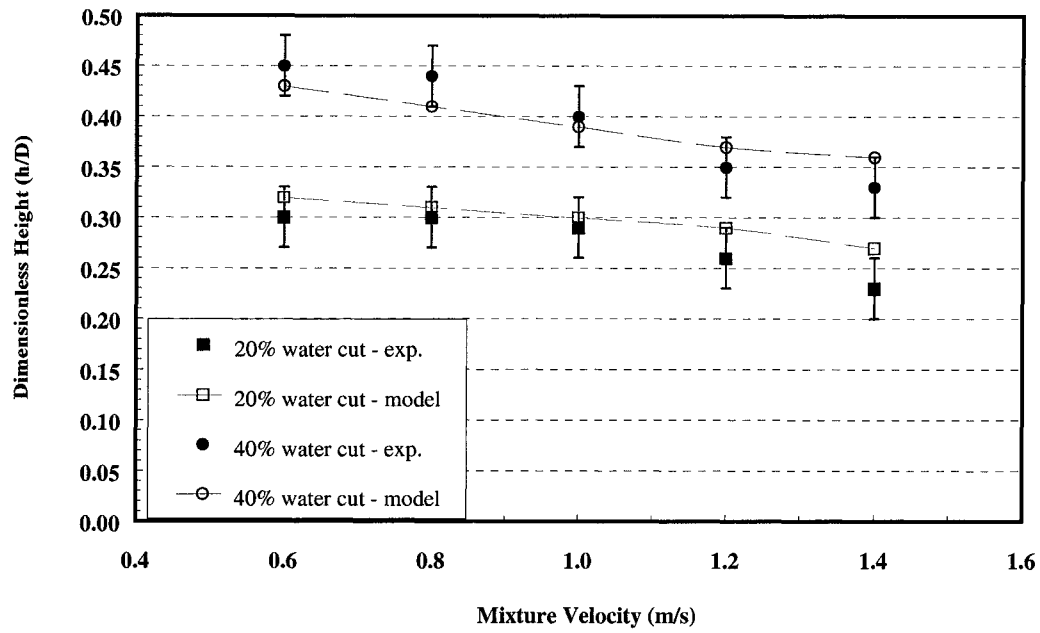


Figure 11 Variation of total water film height with velocity

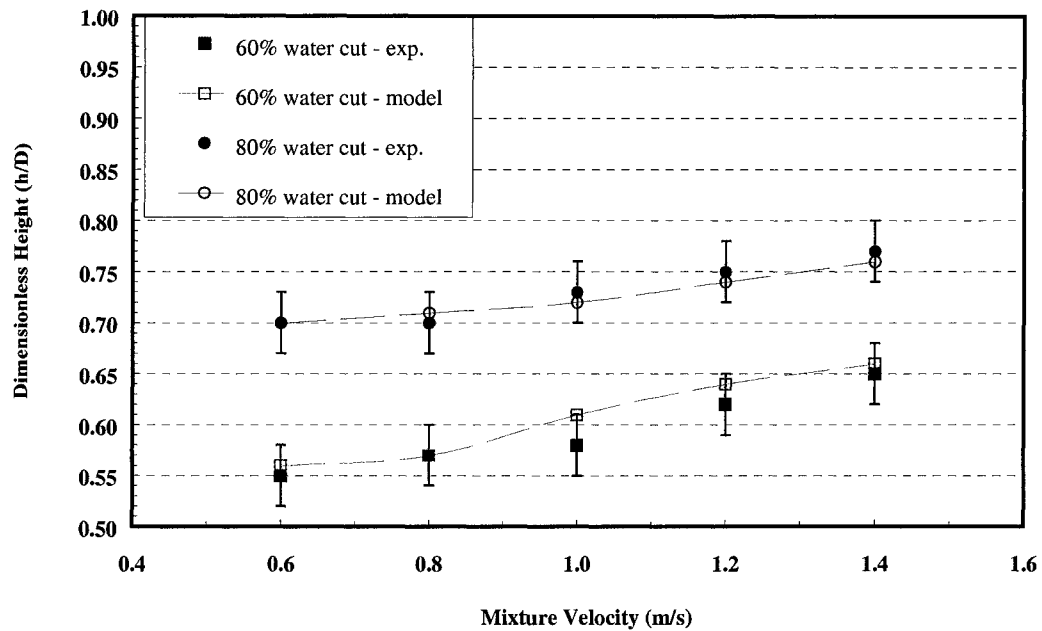


Figure 12 Variation of total water film height with velocity

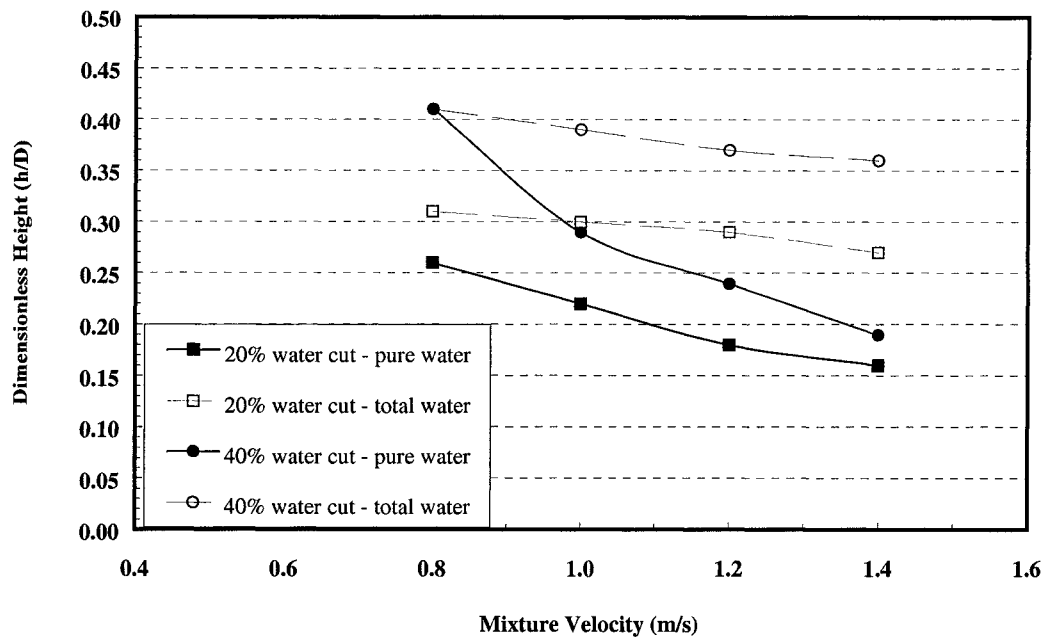


Figure 13 Pure water vs. total water height at different velocities

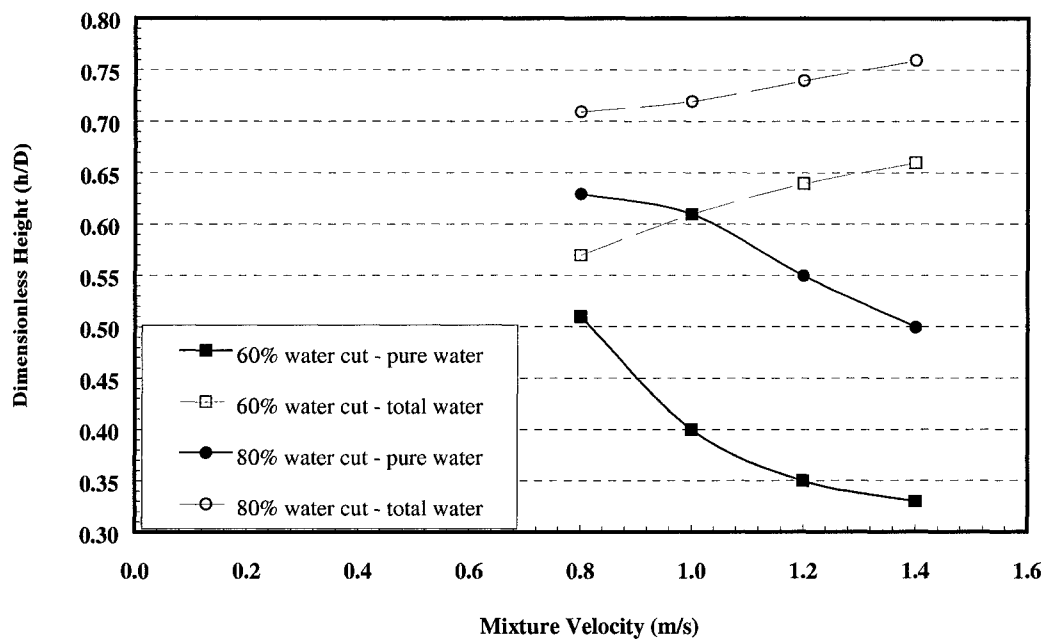


Figure 14 Pure water vs. total water height at different velocities